

# EXAFS Studies of Polymer Electrolytes

R. G. Linford

Department of Chemistry, De Montfort University, The Gateway, Leicester LE1 9BH, U.K.

## 1 Introduction

Extended X-ray Absorption Fine Structure, EXAFS, is a technique which probes the local structure, *i.e.* the nature, number, and distance of near neighbours which surround atoms or ions of a chosen element within a sample. Although it can be applied to crystalline solids for which diffraction is the technique of choice, its real strength lies in elucidating structural aspects of solutions, highly disordered materials, and amorphous solids, which lack the long-range order needed for diffraction studies. Polymer electrolytes are amorphous, ionically conducting materials in which simple ionic salts are dissolved in long-chain heteropolymers such as poly(ethylene oxide), PEO. Typical values of the ratio,  $n$ , of polymer repeat unit to salt in an electrolyte  $\text{PEO}_n\text{:MX}_1$  are in the range 3 to 100.

Structural considerations dictate the behaviour and hence the potential applications of polymer electrolytes. There is therefore a happy complementarity between the technique and the class of materials, which this review explores.

### 1.1 Structural Studies

The majority of structural studies of interest to chemists involve the application of diffraction techniques to crystalline materials which possess long-range order; X-ray and neutron diffraction are much used for elucidating the structure of the bulk as are electron diffraction techniques, especially LEED and RHEED, for investigations of the surface region. Neutron and electron diffraction have not yet been strongly exploited in polymer electrolyte studies. X-Ray diffraction undeniably gives substantially more information<sup>1,2</sup> than the analysis of fine structure in the X-ray absorption spectrum that forms the major theme of this review, but a non-trivial drawback from the perspective of polymer electrolytes is that such information pertains to the crystalline phases whereas *conduction occurs in the amorphous regions*. It is highly likely that structural inferences drawn from studies of the crystalline phase can be meaningfully applied to amorphous regions of similar concentration but it is not obvious that such conclusions would necessarily hold for the more dilute systems that form the basis of useful electrolyte materials.

The structural features of interest for polymer electrolytes therefore need to be addressed by techniques similar to those used to elucidate structural aspects of the other major class of systems lacking long-range order, namely the glasses. These techniques include XAFS (X-ray Absorption Fine Structure) and neutron scattering. The latter has yet to be significantly applied to polymer electrolytes although interesting studies have been carried out on analogous metal salt-oligomer systems.<sup>3</sup> Our focus therefore for the remainder of this review will be on the main region of the XAFS spectrum, the EXAFS (Extended X-ray Absorption Fine Structure) region, although there is also interesting chemical information to be found<sup>4,5</sup> in the edge region and the XANES (X-ray Absorption Near Edge Structure) region.

Polymer electrolytes differ from glasses especially in one respect. A glass is a disordered material below its  $T_g$  (glass transition temperature) and consequently long-chain segmental motion is precluded. It turns out from Raman and Brouillon scattering experiments<sup>6</sup> that, in polymer electrolytes, the ionic motion is coupled to this type of segmental motion and ionic conductivity is only significant above  $T_g$ . Whereas this does not mean that glassy materials cannot form solid electrolytes (indeed, many examples exist<sup>2,7,8</sup>), it follows that a material that is a polymer electrolyte above  $T_g$  cannot be described as such at a lower temperature.

There is obviously complementarity which is now being exploited<sup>9</sup> between techniques such as EXAFS that address the number, nature, and distance of the neighbours to a chosen ion species and those such as IR and Raman spectroscopy<sup>6,10</sup> which reveal vibrational interactions between such a species and its neighbours, and/or perturbations of intramolecular vibrations (*e.g.* in polymer electrolyte anions such as  $\text{CF}_3\text{SO}_3^-$ ) caused by such interactions.

Before discussing in detail the features that make polymer electrolytes such interesting materials, the EXAFS technique will be outlined, with particular emphasis on factors that affect the study of these salt/polymer 'solutions'. Fuller details are given elsewhere.<sup>11</sup>

## 2 Experimental EXAFS

### 2.1 Outline

When a high energy X-ray photon penetrates to the K shell of a target atom or ion, then there is a high probability that the photon will be absorbed and a K photoelectron will be ejected. It is helpful to visualize this as a wave, propagating spherically from the target species. When this wave impinges on a neighbouring atom, it is back-reflected, and the interference between the outgoing and back-reflected waves gives rise to the experimentally observed EXAFS spectrum.

A schematic illustration of the process is shown in Figure 1. A crude two-dimensional analogue of the process occurs when a stone is dropped into a lily pond. The ripples travel outwards towards the lily leaves and are reflected back by them. The interference between outgoing and returning waves contains information about the distance, number, type, and geometric arrangements of the neighbours – lily leaves or atoms depending whether one is performing the conceptual or the actual experiment.

In an EXAFS experiment, an intensely bright beam of monochromatic X-radiation, usually produced from a synchrotron source, hits a sample. If the energy of the incident beam is scanned from about 100 eV ( $1 \text{ eV} = 1.60219 \times 10^{-19} \text{ J}$ ) below to

Roger Linford studied chemistry at Oxford with Lionel Staveley and was an NSF Fellow with Joel Hildebrand at Berkeley, California from 1968–70. He then moved to Berkeley, Gloucestershire as a tribologist with Les Michell in the CEGB Research Laboratories. In 1973 he was appointed Reader in Chemistry at Leicester Polytechnic, now De Montfort University, becoming a Professor in 1987 and subsequently Head of the School of Applied Sciences which contains the Departments of Applied Physics, Biological Sciences, Chemistry, and Pharmaceutical Sciences. He has edited two books on Electrochemical Science and Technology of Polymers.



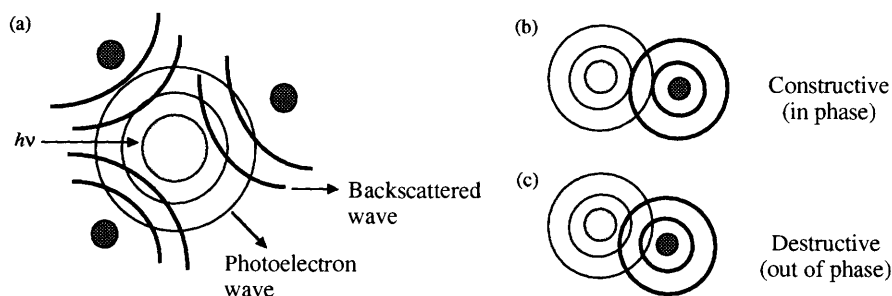


Figure 1 Schematic view of the EXAFS process.

about 1000 eV above a characteristic core electron energy level of a chosen element within the sample, a XAFS spectrum similar to that shown in Figure 2 is produced. The EXAFS information is in the wiggles above the absorption edge. If the background is then properly subtracted, a  $k$ -space EXAFS spectrum is obtained, as in Figure 3, which can be converted into a radial distribution function in real space, Figure 4, by fast Fourier transformation. The fit of these two representations to a trial structure can then be refined by iteration, so that the average number, nature, and distance of neighbours within about 6 Å ( $1 \text{ Å} = 10^{-10} \text{ m}$ ) of the target element species can be ascertained. Distances can be determined much more precisely, usually

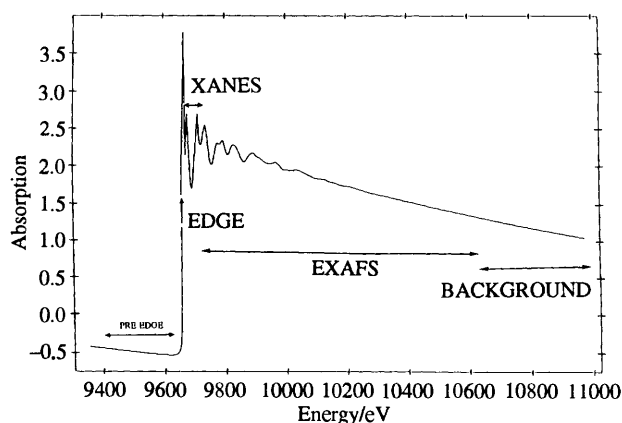


Figure 2 Schematic XAFS spectrum.

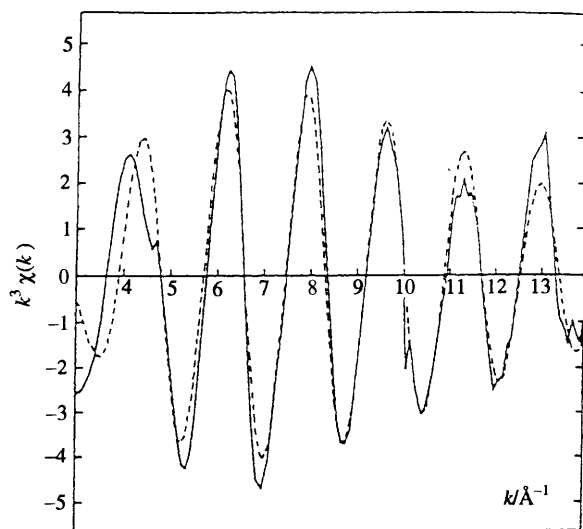


Figure 3 Background subtracted  $k$ -space EXAFS spectrum of  $\text{PEO}_6/\text{ZnCl}_2$ . Experimental data shown as continuous line; theoretical fit shown as dashed line.

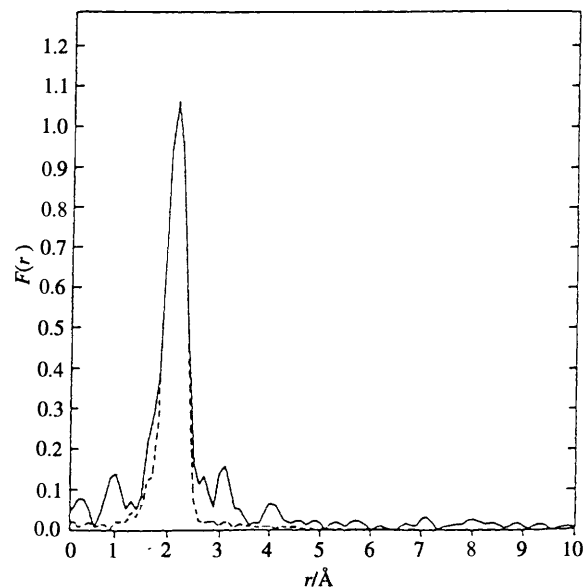


Figure 4 Fast Fourier transform of Figure 3.

within 0.01 Å, than can the number of neighbours which are subject to an error of 10–20%, for reasons outlined in Section 2.3. The implication of this uncertainty in number but not in distance will be discussed in Section 5.

## 2.2 Target Elements

Excitation is normally targeted to the highest cross-section edges which are the K ( $1s$ ) or  $L_{III}$  ( $2p$ ,  $J = 3/2$ ) level of the chosen species. For example, Zn has a K edge at 9659 eV which is well within the range of  $X$ -radiation produced at a dipole bending magnet on a synchrotron ring. Ag has a K edge of 25514 eV which is too high for dipole radiation but which is within the range of a synchrotron device called a wiggler which produces intense bright radiation of higher energies than those that can be obtained from dipoles. Most elements of catalytic interest require wiggler radiation which means that competition for beam time is more severe than for dipole stations, thus restricting the availability of experimental data for polymer electrolytes containing heavy elements. There is considerable present interest in rare earth polymer electrolytes because of their luminescent properties, but these have K-edge energies that are too high (e.g. 53789 eV for Dy) for even a wiggler station and EXAFS above the  $L_{III}$  edge, 7790 eV and thus within the dipole range, has to be used instead. A practical problem that then intervenes is that the  $L_{II}$  edge (at 8581 eV for Dy) is often a little too close to the  $L_{III}$  edge to permit a full post-edge spectrum, including not only the EXAFS region but also the post-edge background, to be collected, which adversely affects the data deconvolution.

Study of elements lighter than Ca or perhaps K requires a greater intensity of soft  $X$ -rays than are produced at a normal dipole station and beamlines located after synchrotron insertion devices such as undulators must be used. For very light target

elements such as C, O, and N, VUV rather than synchrotron rings are required. These are not at present available in the UK which restricts the opportunity to address the local structure around polymer matrix, rather than salt, elements.

The periodic table shown in Figure 5 summarizes the relative degree of accessibility of EXAFS information for different target elements. For neighbouring atoms or ions to the target species, the general principle is ‘the bigger the better’. It can then be very difficult,<sup>12</sup> however, to locate light neighbours such as oxygen in the PEO matrix surrounding a cation such as Zn or Ni, if the counterion is a heavy backscatterer such as I or Br.

### 2.3 EXAFS Function and Parameter Correlations

The EXAFS function  $\chi$  is quite complicated. In its full form, the fact that the photoelectron wave is curved is taken into account and contributions for the scattering of all the neighbouring atoms are incorporated. Even when simplified to a plane wave approximation for a single scattering atom, the expression is:

$$\chi = \sum_j (N_j / k r_j^2) \exp(-2\sigma_j^2 k^2) t_a t_b t_{ps} t_{is}$$

where  $k$  is the magnitude of the photoelectron wave vector;  $t_a$  is an amplitude reduction factor;  $t_b$  is the backscattering amplitude, which depends on the *nature* of the neighbouring atoms;  $t_{ps}$  is a phase shift term,  $\sin(2kr_j + 2\delta + \psi)$ , in which  $2kr_j$  is the phase shift of the electron by the time it returns from the neighbour,  $2\delta$  is the atomic EXAFS phase shift, caused by the passage of the photoelectron through the potential of the emitting atom, and  $\psi$  is the phase of the backscattering factor; and  $t_{is} = \exp(-2r_j/\lambda)$  which accounts for inelastic scattering.

There is a strong correlation between the coordination number  $N_j$  and the Debye–Waller factor  $\sigma^2$ , and also between the shift in edge energy  $\Delta E_o$  and the neighbour distance  $r_j$ . A set of statistical tests leading to the elegant contour representations shown in Figure 6 has been devised by Joyner *et al.*<sup>13</sup> to ascribe a degree of confidence to the parameters derived from EXAFS studies. It should be remembered that the Debye–Waller factor takes account of two components that contribute to the smearing-out of electron density: thermal effects and static disorder. For a polymer electrolyte system, the latter term cannot be neglected and statistical procedures that artificially constrain the Debye–Waller factor to its normally expected range of thermal values, 0.005 to 0.0025 Å<sup>2</sup>, are not always appropriate.<sup>12</sup> The

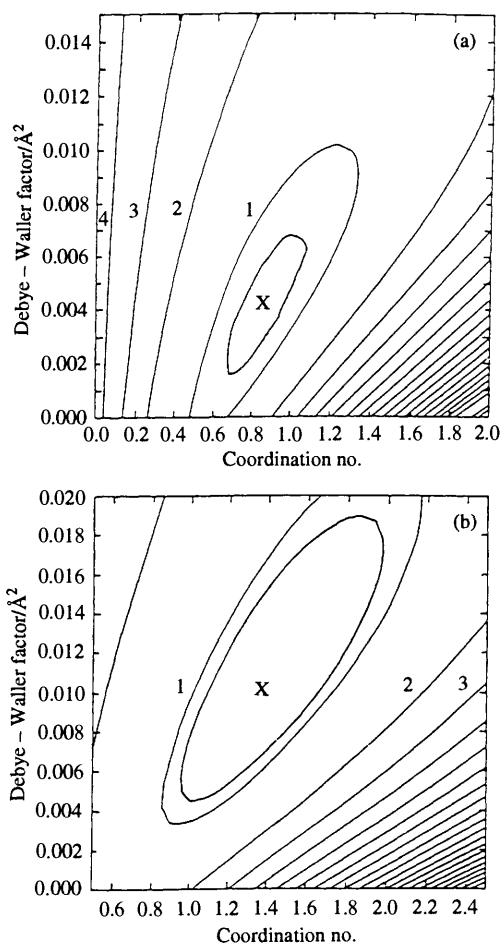


**Figure 6** Contour plots for EXAFS data on  $\text{PEO}_6:\text{ZnCl}_2$ .

10–20% uncertainty in  $N_j$  arises from the correlation between  $N_j$  and  $\sigma^2$ .

The interference effects described above are responsible for the post-edge oscillations in the raw EXAFS spectrum, Figure 2, and in the background-subtracted k-space spectrum, Figure 3. The further away the neighbours are, the closer the oscillations

<b>H</b> 14 -																<b>He</b> 25 -	
<b>Li</b> 55 -	<b>Be</b> 111 -											<b>B</b> 188 -	<b>C</b> 284 -	<b>N</b> 410	<b>O</b> 543	<b>F</b> 697	<b>Ne</b> 870 22
<b>Na</b> 1071 30	<b>Mg</b> 1303 49											<b>Al</b> 1559 73	<b>Si</b> 1839 100	<b>P</b> 2145 135	<b>S</b> 2472 163	<b>Cl</b> 2822 200	<b>Ar</b> 3206 248
<b>K</b> 3608 295	<b>Ca</b> 4038 346	<b>Sc</b> 4492 399	<b>Ti</b> 4966 454	<b>V</b> 5465 512	<b>Cr</b> 5989 574	<b>Mn</b> 6539 639	<b>Fe</b> 7112 707	<b>Co</b> 7709 778	<b>Ni</b> 8333 853	<b>Cu</b> 8979 932	<b>Zn</b> 9659 1022	<b>Ga</b> 10367 1116	<b>Ge</b> 11103 1217	<b>As</b> 11867 1324	<b>Se</b> 12658 1434	<b>Br</b> 13474 1550	<b>Kr</b> 14326 1678
<b>Rb</b> 15200 1804	<b>Sr</b> 16105 1940	<b>Y</b> 17038 2080	<b>Zr</b> 17998 2223	<b>Nb</b> 18986 2371	<b>Mo</b> 20000 2520	<b>Tc</b> 21044 2677	<b>Ru</b> 22117 2838	<b>Rh</b> 23220 3004	<b>Pd</b> 24350 3137	<b>Ay</b> 25514 3351	<b>Cd</b> 26711 3538	<b>In</b> 27940 3730	<b>Sn</b> 29200 3929	<b>Sb</b> 30491 4132	<b>Tc</b> 31814 4341	<b>I</b> 33169 4557	<b>Xe</b> 34561 4786
<b>Cs</b> 35935 5012	<b>Ba</b> 37441 5247	<b>La</b> 38925 5483	<b>Hf</b> 65351 9561	<b>Ta</b> 67416 9881	<b>W</b> 69525 10207	<b>Re</b> 71676 10535	<b>Os</b> 73871 10871	<b>Ir</b> 76111 11215	<b>Pt</b> 78395 11564	<b>Au</b> 80725 11919	<b>Hg</b> 83102 12284	<b>Tl</b> 85530 12658	<b>Pb</b> 88005 13055	<b>Bi</b> 90526 13419	<b>Po</b> 93105 13814	<b>At</b> 95730 14214	<b>Rn</b> 98404 14619
			<b>Ce</b> 40433 5723	<b>Pr</b> 41991 5964	<b>Nd</b> 43569 6208	<b>Pm</b> 45184 6459	<b>Sm</b> 46834 6716	<b>Eu</b> 48519 6977	<b>Gd</b> 50239 7243	<b>Tb</b> 51996 7514	<b>Dy</b> 53996 7790	<b>Ho</b> 55618 8071	<b>Er</b> 57486 8358	<b>Tm</b> 59390 8648	<b>Yb</b> 61332 8944	<b>Lu</b> 63314 9244	

**Figure 5** Periodic table, showing binding energies of K and L<sub>III</sub> shells (upper and lower numbers respectively). K and L<sub>III</sub> energies accessible on a normal dipole synchrotron station are shown in green and yellow respectively; K shell energies for hard X-ray sources (e.g. Wiggler lines) are shown in blue and those accessible by SOXAFS are shown in red.

are to the absorption edge. The XANES region up to 50 eV above the edge contains information about second and third nearest neighbours whereas the ensuing EXAFS region pertains to the nearest neighbours. Beyond the EXAFS region and before the unperturbed post-edge background region is reached, there is a domain of atomic EXAFS, in which further-out electrons within the target atom itself interfere with the outgoing K or L<sub>III</sub> photoelectron.

The XANES region is often called the NEXAFS (Near Edge XAFS) region by American workers. The information that it contains about second and third nearest neighbours is complicated by multiple reflection events from the first neighbour shell. In practice, therefore, it is often easier to interpret XANES spectra in a semi-quantitative and comparative way, and to ascribe particular 'peaks' to the presence of contributing species in different valence states, than to attempt a theoretically rigorous deconvolution.<sup>5</sup>

## 2.4 EXAFS, FLEXAFS, and SEXAFS

Conventional EXAFS is performed in transmission mode. A monochromatic X-ray beam passes through an ionization chamber in which the incident intensity,  $I_0$ , is measured, then through the sample, and finally through a second ionization chamber to measure the transmitted intensity  $I$ . For a sample of thickness  $x$  the absorption coefficient  $\mu$  (which is analogous to the extinction coefficient  $\epsilon$  in the Beer-Lambert relationship) is given by

$$\log(I_0/I) = \mu x$$

As can be seen from Figure 7, after the ejection of the photoelectron, an internal electronic transition takes place, the energy of which can be released either as a fluorescent X-ray photon or an Auger electron. The yields from these secondary processes can be measured by single or multiple detectors located away from the transmission path.

FLEXAFS (fluorescent EXAFS) is used for samples in which the concentration of target species is too low for the difference between  $I$  and  $I_0$  to have sufficient statistical validity. For polymer electrolytes, FLEXAFS is preferred to EXAFS for PEO<sub>*n*</sub>MX<sub>*n*</sub> samples where  $n > 30$ . Surface EXAFS or SEXAFS is used for the study of sample surfaces, since the mean free path of the escaping Auger electrons is short enough to restrict

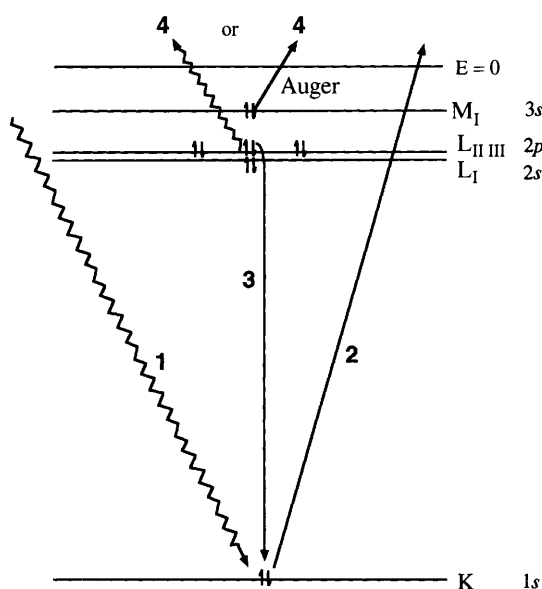


**Figure 7** The photoionization process. Stage 1, incident primary-beam X-ray photon, stage 2, ejection of K photoelectron, stage 3, internal L<sub>II III</sub>→K transition, stage 4, production of K<sub>α</sub> fluorescent X-ray photon or K L<sub>II III</sub> M<sub>I</sub> Auger electron

information to the outermost atomic layers. The full panoply of UHV technology is required for sample study and the duration of an experiment is measured in days or weeks, rather than minutes or hours as for EXAFS or FLEXAFS. SEXAFS has not yet been applied to polymer electrolytes, where its findings might have a bearing on electrode-electrolyte interfacial behaviour, especially with respect to possible phase separation/surface segregation of ionic species.

There are many other acronyms which pertain to EXAFS-related techniques: SOXAFS (soft XAFS) for light elements, REFLEXAFS (reflective FLEXAFS) for glancing angle studies of, *e.g.* electrode/electrolyte interfaces, and QuEXAFS (Quick EXAFS) in which time-dependent processes can be followed. QuEXAFS involves similar instrumentation to EXAFS but the monochromator engineering is more sophisticated. Continuous rather than stepper motors are used and, with better data capture electronics, the equivalent of the one thousand or so sub-millidegree steps that are required to transverse the spectral region shown in Figure 2 can be covered in less than a minute rather than nearly an hour. Energy dispersive techniques in which the full spectral range is covered simultaneously rather than consecutively, have also been used.

## 2.5 Synchrotron Rings

EXAFS features cannot be seen in the X-ray spectrum produced by a normal laboratory X-ray source and a scanning monochromator, although it is possible to produce a passable spectrum from a powerful rotating anode generator for a sample stable enough to withstand exposure times measured in many hours or days. The source of choice is a synchrotron ring and there is a growing number (more than 20) of national and international synchrotron facilities around the World, including three in Japan and new sources shortly to open in Brazil and Australia.

In a typical synchrotron ring, high energy electrons produced in a linear accelerator are further accelerated in a booster synchrotron before being injected into the synchrotron ring itself. This is a large polyhedral stainless steel tube, like a child's train track made up of straight and curves. It is some hundreds of metres in circumference, and the electron beam of 100–200 mA is guided by magnets along a central path. The magnets squeeze the beam into a small, high brightness, cross-section and the ring is under ultra-high vacuum to provide long electron mean free paths and hence a decent ring current lifetime before a further injection of electrons is required. The electrons typically have an energy of 2–6 GeV and are travelling almost at the speed of light. When relativistic electrons accelerate by changing directions (*i.e.* go round a curve), they emit electromagnetic radiation particularly in the X-ray region. The emitted photons pass along beam lines on which experimental stations, configured for various purposes including EXAFS experiments, are located.

The energy range of maximum intensity for a given beamline can be tuned by the incorporation of insertion devices such as undulators (arrays of permanent magnets) located in the preceding straight section of the electron path. Other devices such as wigglers which are powerful (5–6 T) superconducting magnets can also be used to introduce a chicane or Z-bend into the electron path, the higher curvature of which shifts the X-ray beam to the harder energies needed to study the heavier elements shown in Figure 5.

An EXAFS station incorporates a scanning monochromator usually involving double crystal, curved or channel-cut Si(111) or Si(220), together with appropriate photon counting devices and amplifiers and suitable sample holders for studies under controlled atmosphere, temperature, *etc.*

## 2.6 Spectral Deconvolution

A suite of off-line computer programs is typically provided by a national facility or by a major user group to extract the information content from the raw spectrum in a series of stages

removal of glitches arising from imperfections in monochromator crystals, calibration of the energy scale, subtraction of pre- and post-edge background by extrapolation using, *e.g.* splined polynomial functions, fast Fourier transformation of the *k*-space spectrum, Figure 3, into the *r*-space radial distribution function, Figure 4, and iteration of the *k*- and *r*-space representations of a trial structure by successive refinements to secure an acceptable fit to the experimental data. Because EXAFS information pertains to near neighbours at short distances, the information content in the high-*k* region is particularly important. For this reason, a  $k^3$  weighting is often used.

### 3 Polymer Electrolyte Materials

Although very recent evidence<sup>14</sup> has been obtained for the presence of nano-sized aggregates of salt dispersed in the polymer matrix for certain systems such as PEO<sub>8</sub>RbBr, polymer electrolytes normally consist of an inorganic salt dissolved in a suitable polymer matrix. They have been considered<sup>2, 7, 8</sup> for some time to be a very important class of solid electrolytes.

#### 3.1 Solid Electrolytes

These are materials that not only conduct ions (but not electrons) but also retain dimensional stability. The long history of the search for suitable solid electrolytes, to which both Faraday and Nernst made important contributions, has been described elsewhere.<sup>2</sup> Many candidate materials have been considered over the years and suitable electrolytes have often been devised by judicious structural modification of substances that perhaps lack, in their unmodified form, a key attribute that is crucial to their successful application. An interesting example is the set of inorganically<sup>15</sup> – or organically<sup>16</sup> – modified silver or copper iodides. These are compounds that, in their parent form, exhibit spectacular cation conductivity only at high temperature, but which can be modified to provide satisfactory ionic conductivity at room temperature by the incorporation of iodides such as RbI (to give Ag<sub>4</sub>RbI<sub>5</sub>) or 4-methyl-1,4-oxathianum iodide (to produce a Cu<sup>+</sup> solid electrolyte called 'Cumoti').

It is fair to say that, for solid electrolytes, the ionic conduction behaviour depends so intimately on the structure, and especially on the local environment in immediate proximity to the potentially mobile ion species, that a dominant role in elucidating their behaviour is played by structural studies including EXAFS.<sup>2</sup> A consequence of this is that investigation of the structural factors that determine phase stability is very germane to the search for new solid electrolytes with greatly improved performance and stability, for potential use in a range of applications including power sources, electrochromic devices, and sensors. By way of example of the quest for fundamental understanding of phase stability, Frech and co-workers have studied Na<sub>2</sub>SO<sub>4</sub> (which acts as a solid electrolyte in its high temperature phase I polymorph), in which surprisingly small amounts of aliovalent dopants such as Dy<sub>2</sub>(SO<sub>4</sub>)<sub>3</sub> have led to structural rearrangements from phase V, the thermodynamically stable structure at room temperature, to phase I or Phase III. The former requires 3% of M<sup>III</sup> cation and the latter only 0.5%. Recently the EXAFS technique, which has made a significant contribution to the understanding of polymer electrolyte behaviour through its unmatched ability to reveal local structure even in amorphous materials, has been applied to these systems,<sup>10</sup> to determine whether the dopant ions are statistically dispersed or segregated in nanoparticle clusters.

#### 3.2 Ionics and Electrochemistry

The production and study of materials, including solid electrolytes, whose behaviour is perhaps dictated by structural rather than molecular considerations is not the domain of a single discipline. Chemists, physicists, materials scientists, electronic

engineers, and crystallographers all play their part.<sup>2</sup> Whereas the area of electronics is inevitably dominated by physicists and electronic engineers, the newer field of ionics is one in which the approach of the chemist comes to the forefront, indeed, it can be considered as a particular aspect of electrochemistry.

For many years, the major focus of interest in both fundamental and applied electrochemistry was in systems involving liquid electrolytes. The particular features that dominate such systems are charge transfer at the electrode–electrolyte interface and the complications caused by convective and mass-transport processes within the mechanically mobile electrolyte. Electronic conductivity in the electrolyte, loss of electrode–electrolyte contact through expansion or distortion, and propensity to crystallization within the electrolyte layer are usually less significant. Liquid electrolytes formed by dissolving ionic salts in aqueous or non-aqueous solvents, are usually sufficiently dilute to be amenable to conventional (Debye–Hückel–Onsager or simpler) treatment and even molten salts in which the ionic concentration is very high and ion-pairing is prevalent, can be analysed by the Fuoss approach.

By contrast, the field of ionics (which is here considered as comprising the application of solid state electrochemistry) is dominated by the very factors that are secondary in liquid state electrochemistry. The electrolyte itself is of major significance and the balance of consideration in the electrode–electrolyte layer lies less with the charge-transfer processes and more with chemomechanical properties such as the formation of dendrites, passivation layers, and loss of contact area at the interface, than is the case for 'conventional' systems.

#### 3.3 Polymer Electrolytes

In solid electrolytes, convection is precluded and transport through the electrolyte external boundary surface or an internal interface such as a grain boundary, is different from that in the bulk. In normal solid electrolytes, usually only one ionic species is significantly mobile and the matrix, which plays the role taken by the solvent in liquid systems, is rigid.

By contrast, polymer electrolytes represent a fascinating intermediate, in which ions move in a flexible disordered matrix which, however, is constrained against long range migration. The term 'immobile solvent' was informally coined by Armand to describe this situation.<sup>17</sup> Their importance lies beyond just the important but narrow focus within ionics, they are in fact exquisite model systems in which to explore the subtle balance of factors that determines solution behaviour.<sup>18</sup>

This can be seen particularly clearly in the case of PEO-based systems. They can be produced by a variety of methods including cryo-grinding and hot pressing,<sup>7, 19</sup> but the most common method is solution casting. Here, dilute solutions of high molar mass poly(ethylene oxide), (PEO) and a chosen metal salt MX<sub>1</sub>, both in volatile solvents, are mixed or co-dissolved and the solvent is allowed to evaporate in a controlled way. The resultant product is a mechanically strong film of composition PEO<sub>*n*</sub>MX<sub>1</sub>, where *n* refers to the number of formula repeat units of CH<sub>2</sub>–CH<sub>2</sub>–O. In this connection, the similarity between the repeat units of PEO and crown ethers should be noted. The film is thin by chemist's standards (30–150 μm), usually translucent and often hygroscopic, so that storage (and indeed preparation) under dry box conditions is frequently employed to minimize the effect of adventitious or occluded water.

The preparation process here is one in which the salt, whose lattice energy has been overcome by the solvation energy of the original casting solution (in which the solvent is typically acetonitrile, methanol, or ethanol), 'transfers its allegiance' to the polymer solvent.<sup>18</sup> The ease of the solution casting method compared with the alternative dry methods outweighs the risk of solvent retention which can be circumvented by suitable drying procedures.

The energetics for this process are very finely balanced, and the composition of the final film is influenced by a number of considerations. The solubility of salt in polymer is such that the



value of  $n$  cannot usually be higher than about 3. On heating, phase separation (sometimes erroneously called 'salting out' in the ionics field) is not unusual; many of these systems exhibit lower critical solution temperature behaviour for entropic reasons.<sup>7</sup> The phase-separated ionic crystals often remain visible to the eye or under the microscope on cooling. We have recently obtained unpublished evidence, however, from atomic force microscope studies in our laboratories that some systems such as  $\text{PEO}_8\text{:NiBr}_2$ , previously thought to be fully soluble at room temperature, in fact contain microcrystals of phase-separated or undissolved salt when the polymer electrolyte is prepared in the total absence of water.

The separation of two further crystalline phases in semi-crystalline polymer electrolytes such as those discussed so far can often be seen under the polarizing microscope. One is a high melting, salt-rich phase, typically with  $n = 3$  or 4; recent<sup>1</sup> elegant X-ray diffraction studies of these compounds have been used to draw indirect conclusions about structure–property relationships in polymer electrolytes. The other is 'pure' spherulitic PEO.

A minor digression concerning polymer crystallinity is helpful at this stage. It is commonplace to regard most ionic inorganic or organic crystalline materials as being 'perfect', although it is universally realized that such crystals are neither totally pure nor defect-free. These materials are composed of discrete molecular or ionic entities held together by Coulomb forces and they are essentially covalently unbonded or only weakly bonded to each other. There are no *a priori* factors that prevent them from arranging into virtually infinite arrays with 3-dimensional long-range order. Long chain polymers crystallize, however, by chain folding, like a series of hairpins laid side by side, and the folds have a different regularity from that of the straight chain unit cell repeat. Further, the crystalline fibrils or lamellae of folded chains radiate and grow from a central nucleation site in a way that has been compared<sup>18</sup> to 'bobbles on the pom-pom of a ski-hat', inevitably trapping amorphous regions of imperfectly aligned chains between them. The crystalline entities produced in this way are called spherulites and contain amorphous as well as crystalline sub-regions. They are embedded in a matrix of uncrystallized amorphous material and show up as bright domains in a dark background under polarized light. A typical example of a semi-crystalline polymer electrolyte film, in which two types of spherulite can be seen, is shown in Figure 8.

From the above, it is clear that phase behaviour in polymer electrolytes is complicated and the reader will not be surprised that the final morphology of a given film is often dictated by kinetic as much as by thermodynamic factors. In consequence, not too much store should be set by attempts to construct authoritative phase diagrams of these polymer–salt systems.<sup>7,17,18</sup>

It has already been stated that moisture affects polymer electrolyte systems. It may therefore seem perverse that studies



**Figure 8** A semi-crystalline polymer electrolyte film of  $\text{PEO}_8\text{:LiClO}_4$  photographed under crossed polarizers in a polarizing microscope.

have been carried out on films cast from aqueous solution (PEO is exceptional in being a water-soluble polymer) and subsequently scrupulously dried, but such materials faithfully mimic those cast from more 'conventional' solvents.<sup>20</sup>

The description so far has been oriented towards polymer electrolytes formed from PEO but a range of other hetero-polymers, containing groups which can coordinate with metal cations through electron lone pairs, have been used.<sup>7,19,21,22</sup> Poly(ethylene imine), PEI, is a particularly successful example which is sufficiently hydrophobic to minimize water retention, but some salts such as those based on rare earth cations dissolve only with great difficulty. Since it turns out that ion transport in polymer electrolytes occurs in the amorphous regions (as will be discussed in more detail in Section 4.1), considerable enthusiasm developed in the middle of the last decade towards the study of systems based on totally amorphous polymers such as poly(propylene oxide), PPO, until it was realized that the very features that repressed crystallinity (the pendant methyl group in this case) also impeded ionic conduction.

Not all salts dissolve in hetero-polymers. Those that do tend to have soft anions such as those favoured in non-aqueous electrochemistry: triflate,  $\text{CF}_3\text{SO}_3^-$ ; perchlorate,  $\text{ClO}_4^-$ ; tetrafluoroborate,  $\text{BF}_4^-$ ; hexafluoroarsenate,  $\text{AsF}_6^-$ ; and the softer halides  $\text{Cl}^-$ ,  $\text{Br}^-$  and especially  $\text{I}^-$ . The subtle energetic balance to which reference was made at the beginning of this section is between the lattice energy of the salt (lower for soft anion materials) and the solvation energy in the polymer which depends on permittivity. This aspect has been discussed in detail elsewhere.<sup>7,17,18</sup> The relative permittivity (dielectric constant) for PEO is only 5, compared with 72 for water, but it has been pointed out by Latham in a private communication that, within the outer double layer for aqueous systems, dipole orientation leads to a similar permittivity value to that of PEO.

The concentration of polymer to salt is typically in the mole ratio,  $n$ , of 3 to 100 although ultra-dilute systems down to  $n = 5000$  have recently been studied.<sup>23</sup> The low values of  $n$  correspond, in terms of overall composition, to salt mole fractions of up to  $x = 0.25$  and molalities exceeding  $7 \text{ mol dm}^{-3}$ ! In the light of the preceding discussion on phase separation, however, it should be realized that the concentration within the amorphous conducting region may be substantially different. At such high concentrations, however, Debye–Huckel limiting law behaviour is not obeyed! Ion pairing is also to be expected, as for molten salts, and the local structural studies that are reviewed here have complemented a range of electrochemical and spectroscopic studies designed to address this phenomenon.

## 4 History

### 4.1 Accident and Serendipity

Traditionally, polymers were envisaged to be insulators, but the discovery of non-negligible conductivity in contaminated PEO led Binks and Sharples<sup>24</sup> among others in the 1960's to study divalent salt–PEO systems, albeit with no recognition of their future significance as polymer electrolytes. In 1973, a seminal study by Wright and co-workers<sup>25</sup> of the crystalline phase  $\text{PEO}_4\text{:NaI}$  revealed a helical structure in which the polymer was wrapped round the cations. A few years later, Armand<sup>26</sup> who, as a graduate student, initially in Huggins group at Stanford and subsequently with Minier at Grenoble had pioneered intercalation materials for battery applications, introduced the description of such materials as 'polymer solid-electrolytes'.

It is normally considered<sup>21</sup> that it was only after Wright's work that Armand realized that the PEO–salt systems would provide flexible and deformable solid electrolytes that could accommodate the 10–15% volume change that accompanies ion insertion. Private discussions with Armand, however, reveal a richer story which is not widely known. It contains features reminiscent of two famous scientific 'accidents of communication'. The first was a chance conversation, described by Watson in his book on the Double Helix. Watson had been unable to make his geometric representations of the bases fit on the helix

until a New Zealand organic chemist pointed out that an enol form, rather than the keto representation favoured by textbooks of the time, would solve his problem. The second was the attempt in 1933 by Jost and Kay, following a prediction by Pauling, to make  $\text{XeF}_4$ . They were thwarted by a shortage of Xe as their only supply was 600 cm<sup>3</sup> from an old mass spectrometer tube, and a successful climax to the search for noble gas compounds had to await the pioneering work of Bartlett and subsequently Peacock in 1964.

In 1970, while working on new cathode materials in California, Armand realized that he needed an electrolyte in which  $\text{Li}^+$  was mobile and which would accommodate the intercalation volume changes. He spoke with a fellow French graduate student then studying elsewhere in the USA who suggested that a glyme-based system would have the required characteristics. He tried dissolving a lithium salt in the only glyme-based system that was readily to hand, Carbowax 3000, used for GC columns. (High molecular weight PEO was not produced in commercial quantities until its introduction as a pharmaceutical blood clotting agent a year or two later.) The conductivity was negligible and Wright's later work was needed to point the way, had Armand tried either a lighter or a heavier analogue, the story would have been different. In 1978 at the second Symposium of Solid State Ionics, Armand eventually presented the seminal paper<sup>26</sup> on a wide range of PEO alkali metal salt systems that effectively inaugurated the field of polymer electrolytes.

Following the conventions of the solid electrolytes field he assumed that conduction was entirely cationic and took place within the crystalline helices. To polymer chemists this was rather implausible, the received wisdom of their field being that motion required the free volume that could only be found in the amorphous region. Ironically, as pointed out by Neat,<sup>27</sup> Wright wrote<sup>28</sup> in 1975 that 'in order to obtain some understanding of the structure of the amorphous regions, the electrical conductivities of the ionic complexes have been investigated'. It is also interesting to note that in many polymer electrolytes, anionic rather than cationic conduction dominates, and there is often a significant contribution from charged ion clusters.<sup>7, 18, 19</sup>

The temperature dependence of conductivity,  $\sigma$ , for many polymer electrolytes is non-Arrhenius.<sup>7, 19, 21, 22</sup> A plot of  $\log[\sigma]$  or (in the light of the Nernst–Einstein equation and recalling that it is diffusion rather than conduction that is the activated process),  $\log[\sigma T]$  as a function of temperature is curved in accord with the Williams–Landel–Ferry (WLF) or the equivalent Vogel–Tammann–Fulcher (VTF) equation. For WLF/VTF behaviour, conductivity in fact depends on  $T - T_g$ , implying that conduction takes place in the phase that exhibits a glass transition, namely the amorphous region. Although the 'crystalline conduction' concept that dominated the field in its first few years was erroneous, this did not impede the many exciting developments<sup>22</sup> including attempts using plasticisers, fillers *etc.*, to suppress crystallinity, remove the 'knee' in the  $\sigma(T)$  plot, and enhance the room temperature conductivity, that were taking place for technological reasons.

The conceptual breakthrough came at the 4th International Solid State Ionics meeting in Grenoble, five years after Armand had delivered the seminal paper that initiated the field of polymer electrolytes. His colleague Berthier described<sup>29</sup> solid state NMR experiments that unambiguously identified the amorphous, rather than the crystalline, region as the site of the conduction process.

## 4.2 Technology-driven Developments

In Europe, the USA, and later in Japan, the search was on for a viable battery system for electric vehicles. The lead–acid battery, invented in the 1850's and exploited for city centre delivery in London and elsewhere in the 1890's, had been developed virtually to its ultimate form and little further could be done to overcome its inherent theoretical limitation of 200 watt-h/kg, only 40% of which was achievable in practice. What was needed

for a useful vehicle was a range of over 150 miles, a cruising speed of 50–60 m.p.h. and reasonable acceleration and carrying capacity, and this could not be provided by a battery system in which the weight of the lead and the volume of the cell appurtenances represented nearly 50% of the vehicle.

Commercial companies and funding agencies had enjoyed a fifteen year romance with the sodium–sulfur battery. This had a very high energy density, well able to fulfil the expectations of the late 1960's in terms of performance, but in other respects it was a somewhat unlikely choice. It was neither a conventional battery, which has solid electrodes and a liquid electrolyte, nor a solid state battery, in which anode, electrolyte and cathode are all solid. Instead, it had a solid beta alumina electrolyte and electrodes of molten sulfur and molten sodium, and had to be maintained at 350°C during operation. With hindsight, persuading the everyday motorist to enjoy sitting a few feet from such a battery while hurtling to work during rush hour would have been a worthwhile challenge for a marketing department.

By the late 1970's, however, the romance was over, the failure mechanisms in the solid electrolyte seemed insurmountable, and the funding agencies and industry were looking for a new paramour. In the polymer battery, they seemed to have found it. The concept was straightforward: a lithium anode, a Ni current collector attached to an intercalation cathode such as  $\text{Li}_x\text{TiS}_2$  ( $0 \leq x \leq 1$ ) or  $\text{Li}_x\text{V}_6\text{O}_{13}$  ( $0 \leq x \leq 8$ ), and a polymer electrolyte such as  $\text{PEO}_8\text{LiCF}_3\text{SO}_3$  or  $\text{LiClO}_4$  which also acted as a separator. The problem was that, because conductivity was too low below the PEO melting point of 60°C, the cell had to operate at around 120°C. Also, there were problems at the Li–electrolyte interface through passivation and dendrite formation, the former causing a reduction in capacity of 40% within a few charge–discharge cycles and the latter leading to immediate catastrophic failure.

The main European laboratories such as Harwell in England and Riso in Denmark formed large consortia under EEC auspices involving several Universities and many other groups focused their attention on obtaining room temperature conductivity and long-term component stability. But for a curious inversion of serendipity, much of this work would have been restricted by an almost all-embracing patent on the use of polymer electrolyte materials. This covered<sup>30</sup> virtually all metal cations across the periodic table with the exception of the one of focal importance, lithium.

A range of ingenious approaches involving mixed salts, plasticisers, radiation-induced cross-linking, fillers, network, comb and ladder polymers, 'magic' anions such as  $\text{N}(\text{CF}_3\text{SO}_2)_2^-$  have been reviewed elsewhere.<sup>7, 21, 22</sup> We have now reached the stage where systems potentially suitable for commercial traction battery purposes have been developed by General Motors and others. Polymer electrolyte-based alternatives to the non-aqueous lithium batteries using  $\text{LiC}_6$  anodes and  $\text{LiCoCO}_2$  cathodes, which are being produced at the rate of millions per month for portable domestic devices such as camcorders, are also nearing the market place.

## 4.3 Curiosity-driven Research for Other Potential Applications

There is no rival for Li for power source applications. Other ionic devices, however, such as electrochromic and/or smart windows, sensors, thermoluminescent displays *etc.*, depend on a range of specio-specific ions, and polymer electrolytes based on about twenty different metallic cations have been prepared.<sup>18, 19</sup> Many but not all of these are suitable for XAFS investigation of their local structural environment.

Those that are unsuitable have core electron shell energies that are too low, too high, or too close for examination by conveniently available and suitably intense X-ray sources such as synchrotron rings. An increasing amount of local structural information pertaining to a range of anions and cations, especially  $\text{Br}^-$  and first row transition (3d) elements is becoming available and is summarized in Tables 1–6.

This complements spectroscopic, electrochemical and

thermal analysis in elucidating the factors that determine the ionic conductivity in a wide range of polymer electrolyte materials.

## 5 XAFS and Polymer Electrolytes

What has been established so far is that polymer electrolytes, like other solid electrolytes are materials in which an understanding of structure is of paramount importance. Among their particular characteristics, these materials display a propensity towards crystallinity which is in fact prejudicial to conductivity; a tendency, because of their high concentration, to exhibit ion-pairing; and a susceptibility to interference by water which makes their properties dependent on both preparation and storage conditions.

Polymer electrolytes are used in ionic devices, especially polymer batteries, because they are robust and spill-proof. The electrochemically active ion of choice in such cells is  $\text{Li}^+$  because of its combination of high voltage and low mass. Unfortunately, the region of the XAFS spectrum that is most informative in terms of local structure, the EXAFS region, depends on photoelectron production from a target species and the subsequent interference between the photoelectron wave and its backscattered reflection from nearest neighbours. Lithium is inaccessible to EXAFS both as a target species and a backscatterer and many structural studies have therefore been focused on analogue species based on heavier cations. The XANES and edge regions can be informative, however, for systems in which Li is a backscattering species.<sup>5</sup>

Because of the analogy between cation-crown ether systems and polymer electrolytes,<sup>18</sup> the local structure surrounding the cation might well be expected predominantly to show oxygen neighbours, modulated to some extent by anion neighbours if ion pairing or clustering is involved. This is usually the case. The systems of particular interest, however, are those in which, as Sherlock Holmes said of the Hound of the Baskervilles 'the dog did not bark', *i.e.* where more anions need to be present on a charge balance basis than can be accounted for as neighbours. The questions then become: where are the 'excess' anions located; and why? In a few cases, anion EXAFS has been able to address the first part of the question for polymer electrolytes directly, as has X-ray diffraction of the crystalline analogues. The latter can indeed go further<sup>1</sup> and provide lucid reasons for their locations, for example, straddling cations within adjacent helical coils as shown in Figure 9. It must be remembered, however, that the anion locations in the electrochemically interesting amorphous regions cannot be assumed to be the same.

A number of EXAFS studies listed in Tables 1–6 have been carried out on systems involving PEO and its oligomeric analogues. It has been pointed out in a private communication from Latham that the local structure in short-chain systems might well be expected to resemble that in the concentrated PEO systems in which ions are associated with one chain only. By

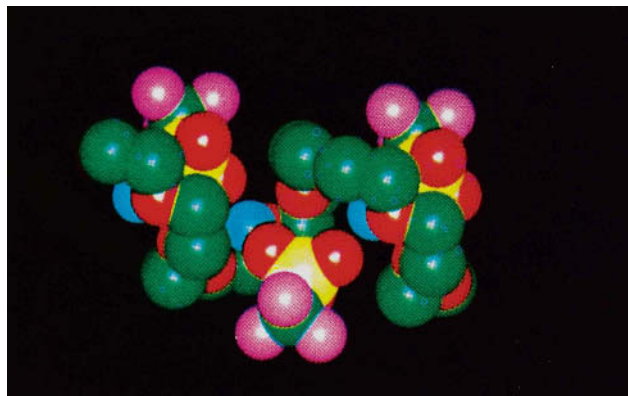


**Figure 9** Crystal structure of  $\text{PEO}_3:\text{LiCF}_3\text{SO}_3$  (with acknowledgements to P. G. Bruce).

contrast, it is normally assumed<sup>7,21</sup> that in more dilute PEO systems there are 'transient cross links' formed by ions attached to more than one chain.

### 5.1 Structure Averaging

EXAFS studies use an incident beam of a few square millimetres in area and the experiments take minutes or hours to perform. The results are therefore averaged over both space and time. For a polymer electrolyte of mixed morphology, in which different regions of a film can be occupied by salt-rich high-melting crystalline spherulites, salt-deficient phase-separated PEO, and the inter-spherulite conducting amorphous region, the spatial averaging can be a problem. In practice, however, the PEO merely acts as an innocuous diluent and investigation can be restricted to films in which the salt-rich crystalline regions are absent. If more than one local environment is present, however, the EXAFS technique usually produces an average structure. The time averaging is not usually a problem for polymer electrolytes as crystallization and other morphological changes are slow. QuEXAFS would be necessary, however, to address local structural changes during the solvent evaporation preparation stage.

### 5.2 EXAFS Studies of Local Structure in Polymer Electrolytes

The seminal investigation was that by Catlow, Chadwick, and co-workers<sup>31</sup> in 1983 on  $\text{PEO}_n:\text{RbI}$  who found each Rb was surrounded by 4 neighbouring oxygens from the PEO chains. There are few other studies of any sort on this particular polymer electrolyte system which differs from the majority in being almost free from a propensity to form crystalline regions but also suffers to an unusual extent from phase separation of salt on heating. Very recent EXAFS studies by McBreen *et al.*<sup>14</sup> have shown that in a similar Rb system,  $\text{PEO}_n:\text{RbBr}$  ( $n = 8, 12$ ), the salt is dispersed in nano-sized aggregates, but that it can dissolve if  $\text{ZnBr}_2$  is also present, as in  $\text{PEO}_{12}:(0.8 \text{ ZnBr}_2 + 0.2 \text{ RbBr})$ .

The choice of a rubidium system was dictated by two main considerations. At that time, despite early work<sup>24</sup> on divalent systems, it was generally accepted, following the key publication of Armand,<sup>26</sup> that useful polymer electrolytes would be confined to those involving alkali metal cations, such as Li, Na, and K. For reasons discussed in detail in Section 2.2, these are not suitable as target atoms for study at a dipole EXAFS station and Rb was chosen instead.

A subtle technicality in fact intruded even with this choice. The number of data points that can be taken in a scan over the EXAFS region, which runs up to about 1000 eV above the absorption edge, depends predominately on two factors: the minimum angular step which can be obtained from the monochromator/stepper motor combination; and the angular range covered, which in turn depends, from the Bragg equation, on the monochromator crystals used. On the only EXAFS station available to those workers at that time, the smallest steps were 1 mdeg and the angular range using Si (220) crystals was only about 0.5 deg. This provided fewer data points than are desirable for optimum deconvolution. This problem is not restricted to Rb, which is the heaviest element usefully accessible to this particular EXAFS facility (station 7.1 at the Daresbury synchrotron radiation source), but also affects Br K-edge EXAFS carried out there, albeit to a lesser extent.

Further studies have been carried out, for example, on the K-edge of the cation<sup>32</sup> and the  $\text{L}_{\text{III}}$  edge of the anion<sup>4</sup> in  $\text{PEO}_4:\text{KI}$  and on the  $\text{L}_{\text{III}}$  edge of the cation in La-based systems.<sup>33</sup> The majority of the remaining EXAFS studies on polymer electrolytes, however, have focused on divalent systems and have been carried out by McBreen's group at Brookhaven,<sup>14,34</sup> or by the author and his colleagues at the Daresbury SRS facility. These are summarized in Tables 1–6.

The data in Table 1 pertain to the local structure surrounding a range of divalent cation species at several stoichiometries. Substantial advances in synchrotron brightness, monochroma-



tor design, background-subtraction methodology, and data deconvolution software have taken place in recent years at Daresbury and these results supercede those from earlier preliminary studies of similar systems by the same workers

The values of coordination number, *N*, and distance, *r*, of neighbouring atoms were those obtained by the refinement procedure outlined in Section 2.6, having regard to the correlations described in Section 2.3 between *r* and  $\Delta E_0$  (which is to some degree a fitting parameter) and between *N* and the Debye-Waller factor  $\sigma^2$ . It is sometimes possible in EXAFS data deconvolution to refine the fits still further by incorporating additional neighbour shells and, to some extent, the choice of neighbour type and the inclusion or otherwise of more than one shell of similar neighbours, is a matter of judgement rather than prescription. It is generally accepted for EXAFS studies that high values of  $\sigma^2$  and  $\Delta E_0$  (or indeed the absence of published values) should be treated with caution. The results presented here are felt to be the best obtainable.

From Table 1 it can be seen that the M–O distance is about 2.1 Å for Co, Ni, Cu, and Zn but is rather larger for Ca. Because the Ca system in particular is very hygroscopic, and since the EXAFS technique is not able to distinguish between neighbouring oxygens from the PEO chains and those from occluded water, scrupulous care was taken to ensure that water was excluded. Special sealable sample holders<sup>3,5</sup> were in fact used for all the studies reported in these tables.

Other trends can be discerned from Table 1. For Co<sup>9,36</sup>, the highly concentrated *n* = 4 system shows a close association between Co<sup>2+</sup> and 4 oxygen atoms together with 2 counterions. This is similar to what would be expected from studies of the crystalline phase for highly concentrated analogous systems.<sup>1</sup> For the more dilute systems the number of Br neighbours, the Co–O distances and the number of O neighbours all decrease

**Table 1** EXAFS of cation K-edges for polymer electrolytes of various stoichiometries

PEO <sub>n</sub> MBr <sub>2</sub> solvent cast	NNA	<i>N</i>	<i>r</i>	$\sigma^2$	<i>E</i> <sub>0</sub>	<i>Ref</i>
<b>M = Co</b>						
<i>n</i> = 4	O	3.8	2.12	0.029	11.92	36
	Br	2.2	2.38	0.010		
<i>n</i> = 8	O	4.0	2.16	0.024	13.64	9
	Br	3.0	2.39	0.015		
<i>n</i> = 15	O	3.6	2.09	0.024	13.70	36
	Br	2.7	2.38	0.013		
<i>n</i> = 30	O	1.9	2.06	0.011	11.36	36
	Br	1.4	2.39	0.008		
<b>M = Ni</b>						
<i>n</i> = 8	O	5.8	2.12	0.027	17.92	9
	Br	4.5	2.40	0.022		
<i>n</i> = 100	O	5.7	2.03	0.017	18.57	37
	Br	—	—	—		
<b>M = Cu</b>						
<i>n</i> = 8	O	1.1	2.02	0.016	12.88	9
	Br	3.2	2.36	0.019		
<b>M = Zn</b>						
<i>n</i> = 8	O	2.2	2.03	0.015	3.14	9
	Br	2.4	2.34	0.008		
<b>M = Ca</b>						
<i>n</i> = 4	O	7.3	2.40	0.028	11.82	38
	Br	1.7	2.83	0.021		
	Ca	1.9	3.38	0.020		
<i>n</i> = 8	O	9.2	2.41	0.030	10.95	38
	Br	2.0	2.78	0.039		
	Ca	2.0	3.35	0.018		
<i>n</i> = 12	O	9.1	2.38	0.024	12.50	38
	Br	1.0	2.83	0.026		
	Ca	2.8	3.36	0.029		

NNA = nearest neighbour atom. *N* = coordination number. *r* = inter atomic distance/Å.  $\sigma^2$  = Debye-Waller factor/Å<sup>2</sup>.  $\Delta E_0$  = difference in eV between value at absorption edge energy from the experimental EXAFS spectrum and that found after data deconvolution.

with dilution. Both the first two trends imply a reduction in Co–Br clustering, thus permitting a closer interaction between cation and polymer chain but the concomitant reduction in number of oxygen neighbours is unexpected. Somewhat different values for Co–O distance (2.49 Å) and number of neighbouring oxygens (6) have been reported<sup>34</sup> for PEO<sub>16</sub>CoBr<sub>2</sub>, perhaps reflecting the gentler drying procedures used in that study. In the Ni systems,<sup>9,37</sup> ion clustering is present in concentrated and absent in dilute systems, and a similar reduction in M–O distance to that observed in Co systems is found.

There are substantial and interesting differences in number of O and Br neighbours for the *n* = 8 systems of the transition metals studied. Whereas Co and Cu each have about 3 Br neighbours on average, Ni has more and Zn has less, and for O neighbours, Ni again shows the most pronounced interaction. These subtle differences reflect the intriguing balance of factors that determine the stability of polymer electrolytes.<sup>18</sup> The Ca systems are much more tightly surrounded by neighbours across the concentration range which leads to very low cation conductivity.<sup>38</sup>

**Table 2** EXAFS of Zn K-edge for zinc halide polymer electrolytes

PEO <sub>8</sub> ZnX <sub>2</sub> Solvent cast	NNA	<i>N</i>	<i>r</i>	$\sigma^2$	<i>E</i> <sub>0</sub>	<i>Ref</i>
X = I	O	3.6	2.11	0.048	5.73	12
	I	1.0	2.51	0.006		
X = Br	O	2.2	2.03	0.015	3.14	9
	Br	2.4	2.34	0.008		
X = Cl	O	1.4	2.05	0.010	7.41	12
	Cl	0.9	2.20	0.004		

NNA = nearest neighbour atom. *N* = coordination number. *r* = inter atomic distance/Å.  $\sigma^2$  = Debye-Waller factor/Å<sup>2</sup>.  $\Delta E_0$  = difference in eV between value at absorption edge energy from the experimental EXAFS spectrum and that found after data deconvolution.

The results<sup>1,2</sup> in Table 2 pertain to the effect on a PEO<sub>8</sub>ZnX<sub>2</sub> system of changing the halide ion. With the large polarizable ions I<sup>−</sup> and Br<sup>−</sup>, there are nearly 4 neighbouring oxygens from the polymer chain but for the Cl<sup>−</sup> system, the numbers of both O and Cl neighbours are very low. There is considerable evidence<sup>9,14</sup> that the PEO<sub>8</sub>ZnBr<sub>2</sub> system contains neutral ZnBr<sub>2</sub> entities.

As is common in materials science, preparation conditions can influence the end product. For polymer electrolytes, the importance of the drying regime has been discussed above, and the effect of different procedures on the local cation structure is summarized in Table 3. Some years ago, a series of comparisons was carried out between systems prepared under two rather different philosophies.<sup>18</sup> Workers at the University of Pennsylvania were anxious to ensure that all traces of water were removed, whatever the consequences might be with respect to polymer morphology, whereas those at Leicester preferred to avoid high temperature drying because of its tendency to encourage the formation of crystalline phases. EXAFS experiments were carried out<sup>20,36</sup> on samples prepared according to both USA (D140) and UK (D50) procedures, for Zn electrolytes cast from water and Co electrolytes cast from acetonitrile.

It can be seen from Table 3 that the number of oxygen neighbours in water-cast samples dried for 7 days at 50°C is anomalously high, indicating that such a drying procedure is not completely successful in removing this relatively involatile casting solvent. By contrast, the D50 and D140 results for solvent-cast Co electrolytes show a similar number of neighbouring oxygens, indicating that volatile solvents can be successfully removed, as can adventitious water. Some results are also presented in the tables for microwave-dried samples<sup>36,39</sup> which

**Table 3** EXAFS of cation K-edge for polymer electrolytes prepared under different drying and casting conditions

Samples	NNA	<i>N</i>	<i>r</i>	$\sigma^2$	$E_0$	Ref
PEO <sub>8</sub> ZnBr <sub>2</sub> Water cast						
Series U	O	2.1	1.99	0.010	6.36	20
	Br	1.7	2.33	0.009		
Series D50	O	5.4	2.17	0.037	10.20	20
	Br	2.3	2.32	0.010		
Series D140	O	3.4	2.14	0.031	6.44	20
	Br	2.1	2.32	0.009		
PEO <sub>8</sub> CoBr <sub>2</sub> Solvent cast						
Series D50	O	4.0	2.16	0.024	13.25	9
	Br	3.0	2.39	0.015		
Series D140	O	4.0	2.11	0.024	12.93	36
	Br	3.1	2.38	0.016		
Series M	O	4.4	2.06	0.032	14.6	36
	Br	2.7	2.37	0.013		
PEO <sub>4</sub> NiBr <sub>2</sub> Water cast						
Series D50	O	2.9	2.07	0.019	10.74	39
	Br	2.5	2.46	0.019		
	O	3.0	2.10	0.031	12.37	39
Series M	Br	3.0	2.46	0.018		
PEO <sub>8</sub> NiBr <sub>2</sub> Solvent cast						
	O	5.8	2.12	0.027	17.92	9
Series D50	Br	4.5	2.40	0.022		

NNA = nearest neighbour atom *N* = coordination number *r* = inter atomic distance/Å  $\sigma^2$  = Debye-Waller factor/Å<sup>2</sup>  $\Delta E_0$  = difference in eV between value at absorption edge energy from the experimental EXAFS spectrum and that found after data deconvolution

U = as cast samples D50 = samples dried at 50°C under vacuum for 7 days

D140 = D50 samples dried at 140°C under vacuum for 2 hours M = samples microwave dried (Hoover Micromaster H 6318) for 2–3 minutes

are broadly similar to those obtained from longer drying regimes

In Table 4, the effect on Zn neighbours of incorporating cations or anions of other species is shown. It can be inferred that Ca and Li bind tightly to the polymer chain,<sup>14,40</sup> since Zn has only Br or I nearest neighbours, no evidence being found for Zn–O interactions in these mixed systems. When Zn is the only cation, however, as in PEO<sub>12</sub> (0.5 ZnBr<sub>2</sub>)(0.5 ZnI<sub>2</sub>), the Zn is surrounded by 4 oxygens and both Br and I are also within the nearest neighbour shell.

The results<sup>35</sup> of Br K-edge EXAFS are reported in Table 5. These results may be compared with those for the Zn K-edge,<sup>9</sup> admittedly at a slightly different stoichiometry and the two sets of results are compatible with the formation of ZnBr<sub>2</sub> entities (each Zn having 2 Br neighbours and each Br having one Zn neighbour) with additional coordination between the cation and the polymer chain.

The effect of temperature on number and distance of nearest neighbours is indicated in Table 6. The PEO<sub>8</sub> ZnBr<sub>2</sub> system was studied<sup>9</sup> at room temperature, the polymer matrix being above its glass transition temperature, and also<sup>41</sup> at –70°C, i.e. below *T*<sub>g</sub> for PEO which is at –60°C, and at –20°C, i.e. below *T*<sub>g</sub> for the polymer electrolyte, which is at –10°C. There is little change in the Debye–Waller factors on moving from an amorphous to a glassy region, indicating that the contribution from disorder is more significant than the thermal term. The number of bromine neighbours decrease on cooling but the Zn–Br distance is unaffected, and there is an accompanying decrease in number and increase in distance for oxygen neighbours.

## 6 Conclusions

For materials such as polymer electrolytes, in which both crystalline and amorphous regions are usually present, the

**Table 4** EXAFS of Zn K-edge for mixed salt polymer electrolytes

Samples	NNA	<i>N</i>	<i>r</i>	$\sigma^2$	$E_0$	Ref
Solvent cast						
PEO <sub>12</sub> (0.5 ZnBr <sub>2</sub> ), (0.5 CaBr <sub>2</sub> )	O				8.33	40
	Br	3.7	2.37	0.013		
PEO <sub>15</sub> (0.5 ZnI <sub>2</sub> ), (0.5 CaI <sub>2</sub> )	O				8.19	40
	I	2.2	2.57	0.003		
PEO <sub>12</sub> (0.5 ZnBr <sub>2</sub> ), (0.5 ZnI <sub>2</sub> )	O	4.1	2.06	0.043	9.60	40
	Br	1.2	2.33	0.012		
	I	0.6	2.51	0.008		
PEO <sub>12</sub> (0.2 ZnBr <sub>2</sub> ) (0.8 LiBr)	Br	4.1	2.42	0.00003	–2.32	14

NNA = nearest neighbour atom *N* = coordination number *r* = inter atomic distance/Å  $\sigma^2$  = Debye-Waller factor/Å<sup>2</sup>  $\Delta E_0$  = difference in eV between value at absorption edge energy from the experimental EXAFS spectrum and that found after data deconvolution

**Table 5** EXAFS of Br K-edge for ZnBr<sub>2</sub> polymer electrolytes

PEO <sub><i>n</i></sub> ZnBr <sub>2</sub>	NNA	<i>N</i>	<i>r</i>	$\sigma^2$	$E_0$	Ref
Solvent cast						
Br K-edge						
<i>n</i> = 12	Zn	0.8	2.33	0.006	8.14	35
<i>n</i> = 15	Zn	0.8	2.33	0.008	9.44	35

NNA = nearest neighbour atom *N* = coordination number *r* = inter atomic distance/Å  $\sigma^2$  = Debye-Waller factor/Å<sup>2</sup>  $\Delta E_0$  = difference in eV between value at absorption edge energy from the experimental EXAFS spectrum and that found after data deconvolution

**Table 6** EXAFS of Zn K-edge for samples at temperatures above *T*<sub>g</sub> (RT), just below *T*<sub>g</sub> for the polymer electrolyte (–20°C) and just below *T*<sub>g</sub> for the parent PEO (–70°C)

PEO <sub>8</sub> ZnBr <sub>2</sub>	NNA	<i>N</i>	<i>r</i>	$\sigma^2$	$E_0$	Ref
Solvent cast						
RT	O	2.2	2.03	0.015	3.41	9
	Br	2.4	2.34	0.009		
–20°C	O	1.3	2.05	0.013	3.67	41
	Br	2.1	2.34	0.009		
–70°C	O	1.6	2.07	0.014	3.79	41
	Br	1.8	2.34	0.006		

NNA = nearest neighbour atom *N* = coordination number *r* = inter atomic distance/Å  $\sigma^2$  = Debye-Waller factor/Å<sup>2</sup>  $\Delta E_0$  = difference in eV between value at absorption edge energy from the experimental EXAFS spectrum and that found after data deconvolution

EXAFS technique can provide useful information about local structure in the amorphous region which is where the processes of scientific and technological interest occur. Helpful structural benchmarks are now being provided<sup>1</sup> by careful diffraction studies of the crystalline regions of high concentration analogues of polymer electrolytes but in the end, the experimentalist has to choose the compromise that is made. Diffraction is precise but cannot access the region of interest, EXAFS is more susceptible to the influence of the experimentalist during the fitting procedure but it is able to ‘speak’ to the amorphous region directly.

**Acknowledgements** I would like to thank Dr R. J. Latham and Dr W. S. Schlindwein for helpful comments and Dr W. S. Schlindwein for preparing the figures and tables.

## 7 References

- 1 P. Lightfoot, M. A. Mehta, and P. G. Bruce, *Science* 1993, **262**, 883.

- 2 R G Linford and S Hackwood, *Chem Rev*, 1981, **81**, 327
- 3 P B Lond, P S Salmon, and D C Champeney, *J Am Chem Soc*, 1991, **113**, 6420
- 4 S G Greenbaum and M L Den Boer, *Mol Cryst Liq Cryst*, 1988, **160**, 339
- 5 M F Toney and J McBreen, *Interface (The Electrochem Soc)*, Spring 1993, 22
- 6 L M Torell, P Jacobsson, D Sidebottom, and G Petersen, *Solid State Ionics*, 1992, **53–56**, 1037
- 7 C A Vincent, in 'Electrochemical Science and Technology of Polymers 2', ed R G Linford, Chapman and Hall, London, 1990, p 47
- 8 P G Bruce, 'Solid State Electrochemistry', Cambridge University Press, Cambridge, U K, 1994
- 9 H M N Bandara, W S Schlindwein, R J Latham, and R G Linford, *J Chem Soc Faraday Trans*, 1994, **90**, 3549
- 10 G Dharmasena, W S Schlindwein, R Frech, and R G Linford, *J Chem Phys*, 1994, **101**, 9232
- 11 B K Teo, 'EXAFS: Basic Principles and Data Analysis', Springer-Verlag, Heidelberg, 1986
- 12 R J Latham, R G Linford, and W S Schlindwein, *Faraday Discuss Chem Soc*, 1989, **88**, 103
- 13 R W Joyner, K J Martin, and R Meehan, *J Phys C*, 1987, **20**, 4005
- 14 J McBreen, X Q Yang, H S Lee, and Y Okamoto, *J Electrochem Soc*, 1995, **142**, 348
- 15 B B Owens and G R Argue, *Science*, 1967, **157**, 308
- 16 R H Dahm, S Hackwood, R G Linford, and J M Pollock, *Nature*, 1978, **272**, 522
- 17 M Armand and M Gauthier, in 'High Conductivity Solid Ionic Conductors', ed T Takahashi, World Scientific, Singapore, 1989, p 114
- 18 G C Farrington and R G Linford, in 'Polymer Electrolyte Reviews 2', ed J R McCallum and C A Vincent, Chapman and Hall, London, 1990, p 225
- 19 C A Vincent and P G Bruce, *J Chem Soc Faraday Trans*, 1993, **89**, 3187
- 20 A G Einset, W S Schlindwein, R J Latham, R G Linford, and R Pynenburg, *J Electrochem Soc*, 1991, **138**, 1569
- 21 R G Linford, in 'Conducting Polymers', ed B Scrosati, Chapman and Hall, London, 1994, p 1
- 22 J Owen, in 'Electrochemical Science and Technology of Polymers 1', ed R G Linford, Chapman and Hall, London, 1987 p 45
- 23 M Aziz, R J Latham, R G Linford, and W S Schlindwein, *Electrochim Acta*, 1995, in press
- 24 A E Binks and A Sharples, *J Polym Sci*, 1968, **6**, 407
- 25 D E Fenton, J M Parker, and P V Wright, *Polymer*, 1973, **14**, 313
- 26 M B Armand, J M Chabagno, and M J Duclot, Second Int Conf on Solid Electrolytes, St Andrews, Scotland, 1978, Abstract No 6 5, M B Armand, J M Chabagno, and M J Duclot, in 'Fast Ion Transport in Solids', ed P Vashishta, J N Mundy, and G K Shenoy, Elsevier North-Holland, New York, 1979, p 131
- 27 R J Neat, Ph D Thesis, De Montfort University, formerly Leicester Polytechnic, 1988
- 28 P V Wright, *Br Polym J*, 1975, **7**, 319
- 29 C Berthier, W Gorecki, M Minier, M B Armand, J M Chabagno, and P Rigaud, *Solid State Ionics*, 1983, **11**, 91
- 30 R E Whetton, Br Patent No 35990/76
- 31 C R A Catlow, A V Chadwick, G N Greaves, L M Moroney, and M R Worboys, *Solid State Ionics*, 1983, **9 & 10**, 1107
- 32 W Q Yang, J Chen, T A Skotheim, Y Okamoto, and M L Den Boer, in Second International Symposium on Polymer Electrolytes, ed B Scrosati, Elsevier Applied Sciences, London and New York, 1989, p 17
- 33 A Bernson and J Lingren, *Electrochim Acta*, 1995, in press
- 34 J McBreen, *Electrochim Acta*, 1995, in press
- 35 M Cole, M H Sheldon, M D Glasse, R J Latham, and R G Linford, *Appl Phys A*, 1989, **49**, 249
- 36 W S Schlindwein, R Pynenburg, R J Latham, and R G Linford, *Nucl Instrum Methods Phys Res B*, 1995, **97**, 292
- 37 R J Latham, R G Linford, R A J Pynenburg, W S Schlindwein, and G C Farrington, *J Chem Soc Faraday Trans*, 1993, **89**, 349
- 38 H M N Bandara, R G Linford, R J Latham, and W S Schlindwein, *Mat Res Soc Symp Proc* 1995, in press
- 39 R J Latham, R G Linford, and R A J Pynenburg, *Solid State Ionics*, 1993, **60**, 105
- 40 R J Latham, R G Linford, R A J Pynenburg, and W S Schlindwein, *Electrochim Acta*, 1992, **37**, 1529
- 41 M D Glasse, R J Latham, R G Linford, and R A J Pynenburg, *Solid State Ionics*, 1992, **53–56**, 1111